Measurement of a Filter Using a Power Detector

N. Vasudev and Oliver M. Collins, *Fellow, IEEE*

***Abstract*—This paper presents experimental results on the measurement of the magnitude and phase response of RF and baseband signal paths made with a power detector. The frequency response is obtained by measuring the magnitude and phase of the output of the power detector when the forward path is excited by a pair of tones. This technique provides a means for making vector measurements using a scalar detector. Instruments, like network analyzers, commonly use a mixer and sinusoidal source to downconvert the signal for digitization and measurement. The downconversion in this paper is performed using a power detector and an extra tone in the excitation signal itself, drastically reducing hardware complexity. Important applications of this technique include the characterization of the digital-to-antenna path of a software radio and the equalization of the antialiasing filter in a wide-band arbitrary waveform generator. Three examples of measurement, one at low frequency and two others at radio frequencies, show that the errors in the measured response are comparable to those obtained using conventional network analyzers.**

***Index Terms*—Equalization, filter measurement, phase response, scalar detector.**

I. Introduction

THIS PAPER examines a technique for the measurement of the forward-path magnitude and phase of an instrument or transmission system. Knowledge of the forward path will usually be used to equalize it so that it becomes linear phase and constant magnitude. If the forward path were time invariant, measurement and equalization at the time of manufacture would be sufficient; however, the analog components in the signal path vary slowly with temperature and time. Hence, some type of built-in system of measurement and equalization is required.

The forward path may be baseband, e.g., a simple digital-to-analog converter (DAC) [1]–[3], or RF, i.e., involving one or more stages of heterodyne upconversion, or at optical frequencies, e.g., a laser source combined with a modulator. Some common examples of the need for forward-path equalization are the antialiasing filter in an arbitrary waveform generator; the DAC–filter-upconversion chain preceding an amplifier that is compensated by a digital predistorter and linear optical modulators. An arbitrary waveform generator requires equalization because the user wants to have a precise known relation between the analog waveform and the digital samples. Amplifier linearization also requires forward-path equalization because it becomes tremendously more difficult if there are unknown magnitude and phase components in the signal path [4]. Linear optical modulators require equalization to prevent pulse dispersion, i.e., they have to be linear phase.

Manuscript received June 1, 2001.

N. Vasudev is with Stryker Endoscopy, San Jose, CA 95051 USA.

O. M. Collins is with the Department of Electrical Engineering, University of Notre Dame, Notre Dame, IN 56556 USA.

Publisher Item Identifier 10.1109/TMTT.2002.802320.

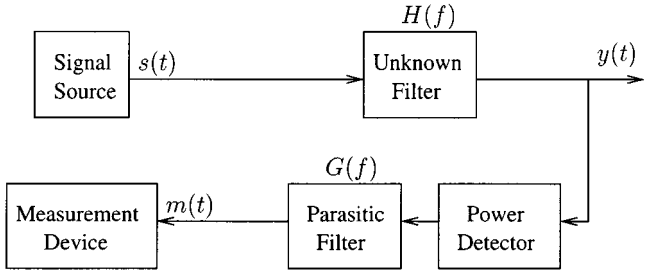

Fig. 1. Measurement using a power detector.

Most instruments that measure filters, e.g., network analyzers, do not have a flat-magnitude linear-phase-output signal path. They merely perform a calibration procedure in which the combined response of the transmitter and receiver is measured. The effect of the combination is removed from subsequent measurements on the device-under-test. Thus, a network analyzer is neither sufficient by itself to solve the forward-path equalization problem, nor is it practical to include a network analyzer in a cell phone base station or an arbitrary waveform generator. A calibrated receiver, e.g., a superior version of the HP89441a fast Fourier transform (FFT) analyzer, will solve the problem; however, there is a classic "chicken and egg" problem of which to calibrate first—the transmitter or receiver.

If only the forward-path magnitude response is to be equalized, a power detector will adequately solve the problem. Scalar network analyzers use power detectors to measure the magnitude response of high-frequency devices across many octaves of bandwidth (BW). Such instruments transmit an AM tone and synchronously detect the signal from the power detector at the modulating tone's frequency. They calibrate the power detector and its associated low-frequency signal path using a source whose power is known so that they can obtain absolute magnitude measurements. These instruments assume that the unknown filters that are being measured do not vary over the AM BW (of the order of tens of kilohertz). Initially, it seems that a power detector makes the determination of phase impossible; however, the overall phase response can be determined by transmitting multiple sinusoids and observing the phases of the beat notes. These tones contain information about the difference of the phases of the sinusoids. Section II explains how information from these sets of exciting tones can be assembled to obtain the overall phase response.

II. Phase From a Power Detector

The most obvious approach to obtaining the phase response is to measure the phase differences for adjacent pairs of a set of equispaced tones and obtain the absolute phase by accumulation of the phase differences. This approach is employed in [5] to characterize the phase of a high-repetition rate laser. Unfortunately,

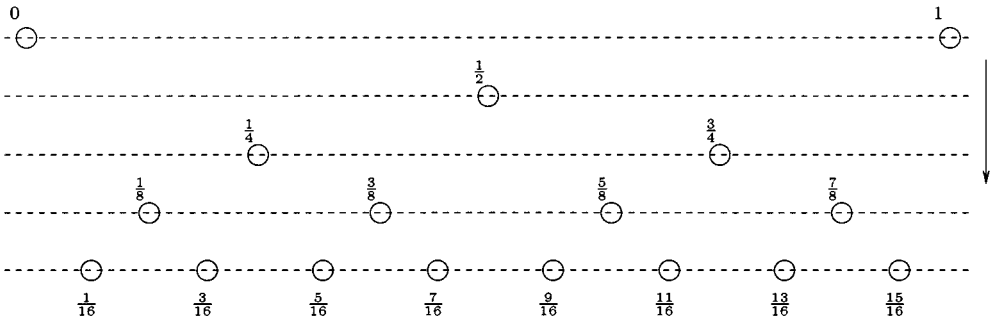

Fig. 2. Order of measurement for the web algorithm.

phase error resulting from the measurements is cumulative, the maximum being proportional to the total number of measurements. Thus, as finer frequency resolution of the phase response is required, the phase error becomes larger. This problem can be solved by making phase-difference measurements between frequencies that are not spaced equally apart.

Unfortunately, this choice exposes some annoying nonideal aspects of power detectors. Obviously, in practical power detectors, there are small variations in magnitude and relatively smaller variations in phase at the output when a pair of tones is swept all the way from dc to many gigahertz. These variations are small over BWs of many octaves at low frequencies and hundreds of megahertz at high carrier frequencies; the parasitics being small at low frequencies and of insufficient Q to create rapid variations at high frequencies. However, large variations in magnitude and phase are obtained when the frequency spacing between the tones is varied at a given carrier frequency. These observations are reflected in the model shown in Fig. 1. The unknown forward signal path is represented by $H(f)$ and the low-frequency variations by $G(f)$.

The calibration of $G(f)$ requires a source whose response is completely known as a function of frequency to an extent better than the source that is being built. Hence, the measurement has to be made assuming no knowledge of $G(f)$. An uncalibrated $G(f)$ prevents the measurement of absolute magnitude, absolute phase, and group delay of $H(f)$. In most systems, e.g., arbitrary waveform generators, DAC-filter-upconversion chains and optical modulators, it is sufficient to make the forward-path linear phase and constant magnitude. Under these conditions, the determination of $G(f)$ is unnecessary.

The phase-measurement algorithm applied in this paper is derived and analyzed in [6]. The graph representation of this algorithm looks like a web and, thus, it is referred to as the web algorithm. The phase at the endpoints of the frequency band are provided as the initial condition to the algorithm. Since only deviations from linear phase are of interest, there is no loss of generality in setting them to zero. The algorithm always uses two phase-difference measurements to obtain the phase at the frequency midway between two frequencies at which the phase is known. Since the phase at the endpoints is known, the phase at the midpoint of the band is measured first. At that time, the phase response at three points in the band is known and this information is used to obtain two more points and so on. Fig. 2 shows the order of measurement of the response progressing from top to bottom on a frequency scale normalized to $(0, 1)$.

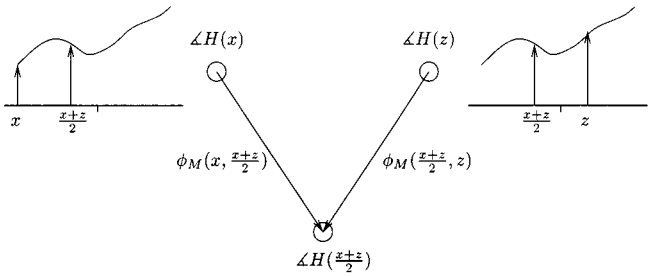

Fig. 3. Algorithm description.

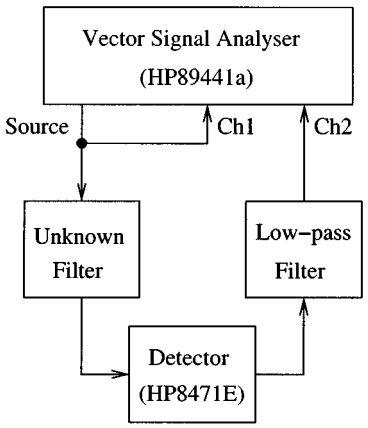

Fig. 4. Measurement configuration.

It can be seen that the midpoints of the frequencies at which the phase is known, overlap; e.g., 3/8 is the midpoint of 0 and 3/4 and 1/4 and 1/2. The algorithm chooses one of the endpoints ("0" or "1" in Fig. 2) as a known frequency point while the second point will be an endpoint in the first step of the algorithm and a point at which the phase has been previously measured in all subsequent steps. Sufficiently many iterations of the algorithm can provide any measurement resolution required. Moreover, it is shown in [6] that the error variance of the phase response found using the web algorithm as a result of independently random measurement errors is less than two-thirds the variance of each phase measurement irrespective of frequency resolution. The growth in the worst-case error is similarly benign, i.e., it can be bounded by a constant.

Fig. 3 illustrates the measurement of the phase at the midpoint of two frequencies x and z, at which the phase response $\angle H(x)$ and $\angle H(z)$, respectively, is known. Two phase-difference measurements are made to obtain $H((x+z)/2)$. The first

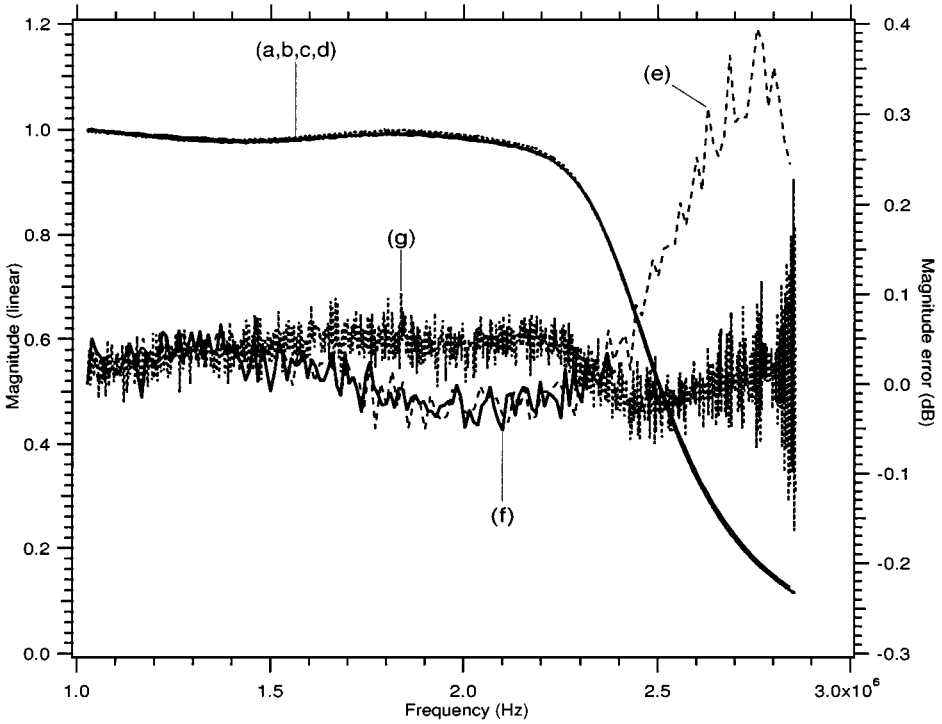

Fig. 5. Magnitude response of 1.9-MHz Mini Circuits LPF. (a) Web algorithm 1.1–2.8 MHz. (b) Web algorithm 1.1–2.4 MHz. (c) HP8753E. (d) HP89441a. (e) (a)/(d) (- - -). (f) (b)/(d) (—). (g) (c)/(d) (· · ·).

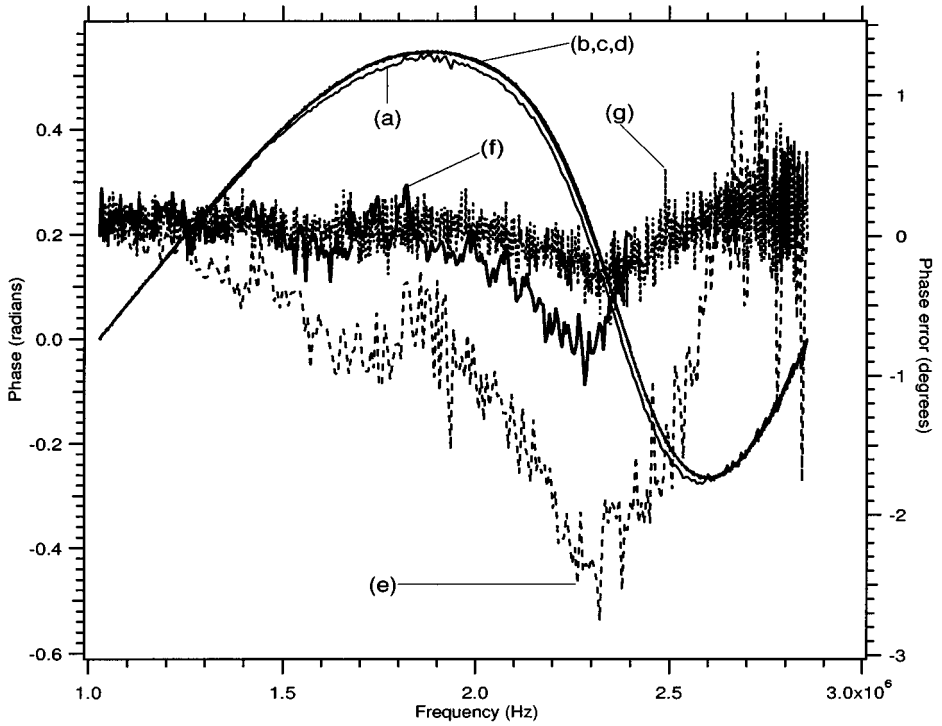

Fig. 6. Phase response of 1.9-MHz Mini Circuits LPF. (a) Web algorithm 1.1–2.8 MHz. (b) Web algorithm 1.1–2.4 MHz. (c) HP8753E. (d) HP89441a. (e) (a)–(d) (- - -). (f) (b)–(d) (—). (g) (c)/(d) (· · ·).

measurement, represented by $\phi_M(x,(x+z)/2)$, is the phase of the sinusoid at the beat frequency $(x-z)/2$ present in the output of the power detector, when tones at x and $(x+z)/2$ are transmitted through the filter $H(f)$. The second measurement $\phi_M((x+z)/2,z)$ is the phase of the sinusoid at the same beat frequency in the power detector's output, when tones at $(x+z)/2$ and z are transmitted through the filter $H(f)$. The error introduced by $G(f)$ is a function of the beat frequency $(x-z)/2$ and is common to both the measurements. This error is removed by the subtraction of the two measurements. The

phase at the midpoint is given by (1).

$$\angle H\left(\frac{x+z}{2}\right)=\frac{1}{2}\left\{\phi_M\left(x,\frac{x+z}{2}\right)-\phi_M\left(\frac{x+z}{2},z\right)\right\}+\frac{1}{2}\Big\{\angle H(x)+\angle H(z)\Big\}. \quad (1)$$

The magnitude response is also measured using a similar web algorithm derived and analyzed in [6].

Section III discusses some practical issues of implementing the web algorithm. Section IV presents an application of the web algorithm to measure a 1.9-MHz Mini Circuits low-pass filter (LPF). Section V describes the measurement of a 100-MHz bandpass filter with a BW of 6 MHz using the web algorithm and Section VI discusses the measurement of an 895-MHz bandpass filter.

III. Practical Issues

The basic step in the web algorithm is the transmission of a pair of tones at frequencies x and y and the measurement of the magnitude $A_M(x,y)$ and phase $\phi_M(x,y)$ of the output of the power detector at the beat frequency $(x-y)$. Synchronous detection of the beat frequency of the power detector's output gives (2), where T_s is the sampling period, $m(i)$ is the sampled power detector output, and N is the total number of samples [chosen to contain an integral number of periods of the sinusoid at frequency $(x-y)$]

$$A_M(x,y)e^{j\phi_M(x,y)}=\frac{1}{N}\sum_{i=0}^{N-1}m(i)e^{j2\pi(x-y)T_s i/N}. \quad (2)$$

The detection can be performed as an FFT, but the sign of the imaginary term has to be appropriately changed. Conversion of the complex number from Cartesian to polar coordinates (A_M and ϕ_M) leads to an ambiguity of 2π in ϕ_M, i.e., $e^{j\phi_M}=e^{j(\phi_M+2\pi i)}$, $\forall i \in$ integers. As the phase response depends on half the measured phase value [see (1)], the phase ambiguity is π. If the range of the phase deviation from linear phase that is being measured is known to within π, the appropriate value can easily be chosen. In cases where a filter is completely unknown, a two-tone sweep can be used to find an initial estimate and then the web algorithm can be employed to obtain the response with both high accuracy and high resolution. Most practical systems employing this measurement technique will have a quite accurately known initial response, i.e., the measurements are required to compensate for changes caused by temperature variations or aging. Hence, the deviations in phase will be well within the range $\{-\pi/2,\pi/2\}$.

Unfortunately, $G(f)$ is not the only complicating factor in a power detector; power detectors are not ideal square-law devices. The common flaws encountered in a power detector are input signal leakage and significant third-order and higher order nonlinearity terms. The nonlinear function of a power detector can be represented by a polynomial $\sum_{i=0}a_i z^i$. The constant term a_0 represents the bias, a_1 represents the signal leakage, a_2 is the desired square-law gain, while a_i, $i>2$ represent higher order coefficients. When a pair of tones is transmitted through such a detector, the output consists of many spurious tones of substantial magnitude, apart from the tone at beat frequency that is being measured. The tone at beat frequency is the result of only the even-order terms in the polynomial expansion of the power detector's function; the odd-order terms generate no power at beat frequency. The even higher order terms do not affect the phase at the beat frequency, even though they do affect the magnitude measurement. Thus, there is often no problem using high-power signals to measure phase response. However, as in scalar network analyzers, generating accurate amplitude data requires that the excitation signal be small enough so that the square-law term dominates.

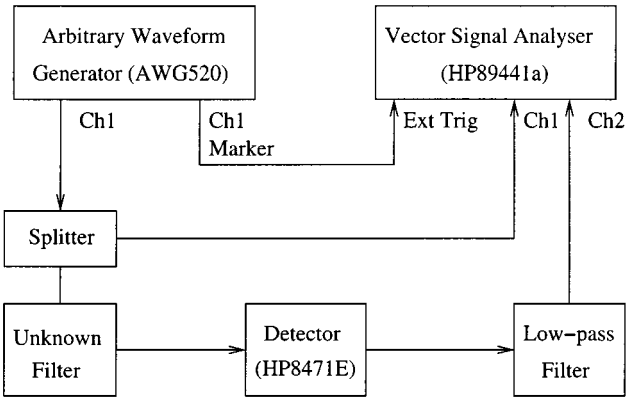

Fig. 7. High frequency measurement configuration.

Phase errors can, however, be produced by poor choice of exciting signals, e.g., if $y=2x$ or vice versa, then the beat frequency overlaps with one of the exciting signals resulting in a large phase error. Smaller errors are produced by overlap with other significant, but smaller magnitude intermodulation products. All such errors can, however, be eliminated by making the ratio of x and y irrational. This ratio can be made irrational for all measurements when the endpoints of the frequency band and their ratio are chosen to be irrational. This goal can be only approximated in a digital system.

Extremely close large spurious tones will cause problems for the synchronous detection in (2), i.e., if the averaging time is small, then leakage from a large close in tone will corrupt the measurement. The introduction of an appropriate window function can mitigate this effect.

Thus, careful thought needs to be given to the set of exciting tones for baseband measurement. Fortunately, in high-frequency bandpass-filter measurements, signal leakage and most of the spurious signals generated by higher order coefficients do not cause problems because they fall far away from the beat frequency and, thus, problems are unlikely to occur. Sections IV–VI discuss three examples of filter measurement. Section IV illustrates baseband filter measurement, while Sections V and VI discuss bandpass filter measurements at 100 and 895 MHz, respectively.

IV. Example 1

This example illustrates the measurement of a 1.9-MHz Mini Circuits LPF. The measurement setup used is shown in Fig. 4. The vector signal analyzer (HP89441a) is both the excitation source and the measuring device. The measurements are logged in the internal RAM of the analyzer and processed using a PC. The source is compensated using the measurement on channel #1, while output of the power detector is measured using channel #2.

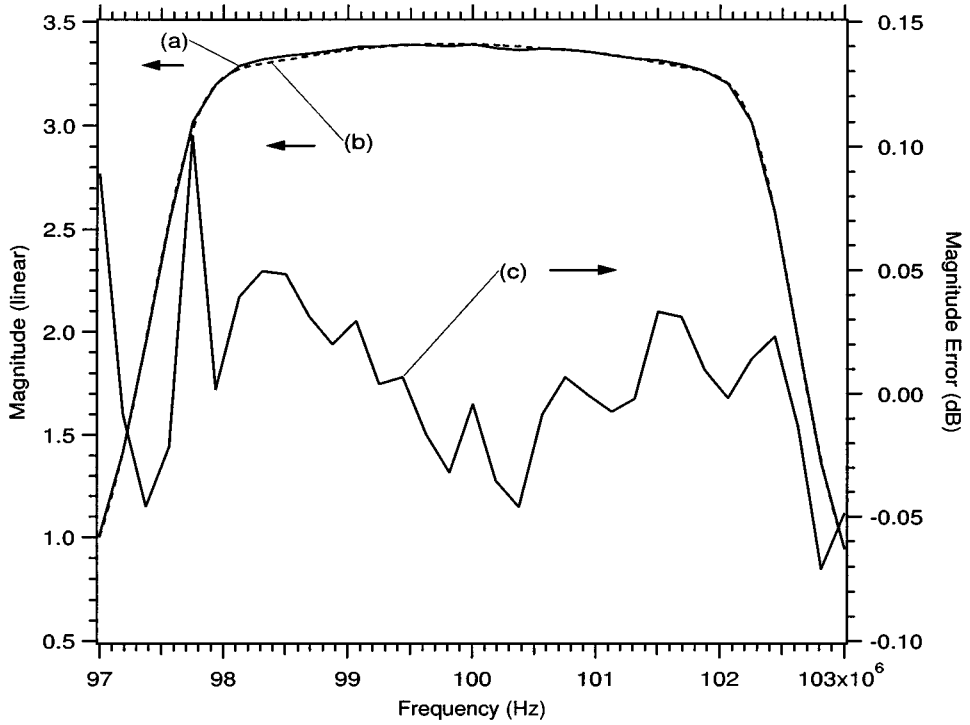

Fig. 8. Magnitude response of 100 MHz K & L bandpass filter. (a) Web algorithm (—). (b) Network analyzer HP4396B (- - -). (c) (a)/(b).

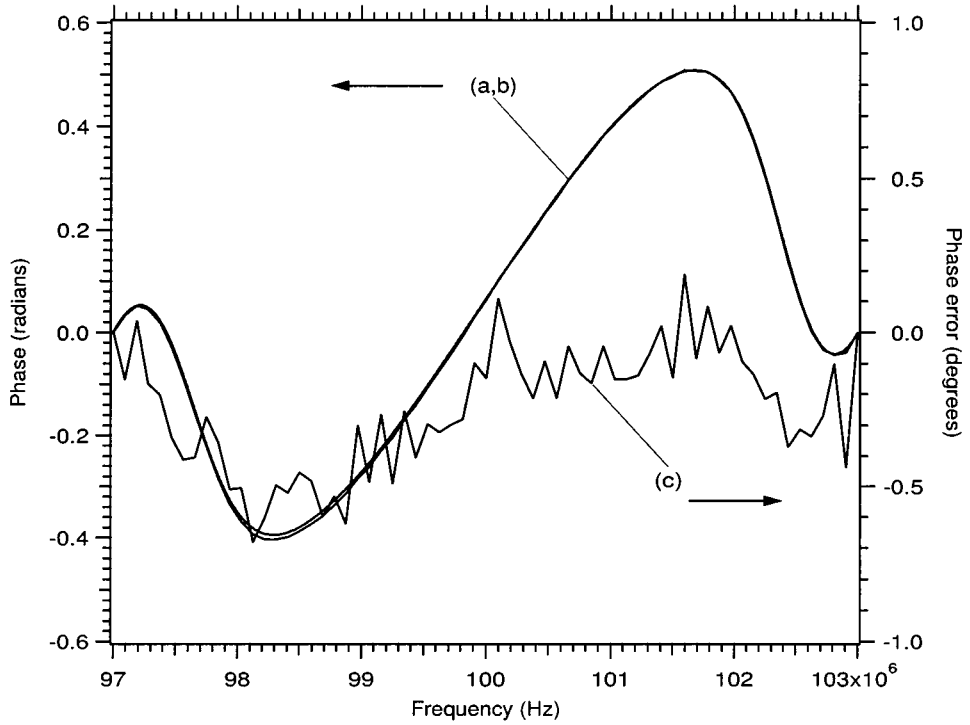

Fig. 9. Phase response of 100 MHz K & L bandpass filter. (a) Web algorithm. (b) Network analyzer HP4396B. (c) Difference (a)–(b).

The vector signal analyzer is programmed to generate pairs of tones (at x and y) and obtain the FFT at frequencies x and y on channel #1, represented by $S(x)$ and $S(y)$, respectively, and at the beat frequency $(x-y)$, represented by $M(x,y)$ on channel #2. The web algorithm determines the frequencies x and y for each measurement. The source compensated measurement, given by $M(x,y)/(S(x)S^*(y))$, is used by the web algorithm to find the phase and magnitude response of the filter. This source compensation eliminates the effects of the terminating impedance when the filter is measured by different instruments.

Figs. 5 and 6 show the magnitude and phase response, respectively, of a Mini Circuits 1.9-MHz LPF. The measurements are made in the BW 1.1–2.8 MHz, which contains the knee of the LPF. The 20-dB point occurs at approximately 2.8 MHz, while the 3-dB point occurs at 2.4 MHz. Traces (a), (c), and (d) refer to the responses measured until the 20-dB point, while (b) is obtained until the 3-dB point. Traces (a) and (b) were ob-

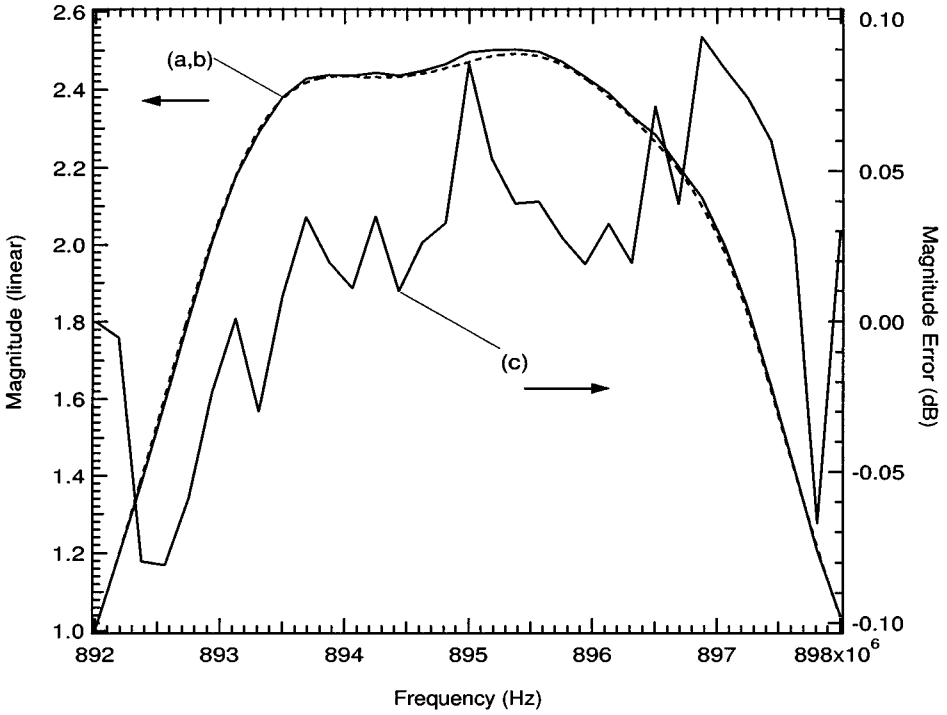

Fig. 10. Magnitude response of 895-MHz K & L bandpass filter. (a) Web algorithm (—). (b) Network analyzer HP8753E (- - -). (c) (a)/(b).

tained using the web algorithm, while (c) and (d) were obtained using a network analyzer (HP8753E) and the vector signal analyzer (HP89441a), respectively. The zero-phase zero-group-delay phase response, shown as (c) and (d) in Fig. 6, is obtained by subtracting a straight line representing a constant phase and group delay from the data obtained from the instruments. For visual comparison of the errors caused by the web algorithm, the initial phase at the 3-dB point for (b) is chosen to be equal to that of (c) at 2.4 MHz, while the phase at the endpoints is zero for (a), (c), and (d). The magnitude response is scaled to unity at 1.1 MHz for all measurements. Each response is shown at 64 points in the respective frequency band. The network analyzer is configured to measure the response at 1600 points and average the spectrum over 16 measurements. The vector signal analyzer measures the response at 3200 points and is configured to average the spectrum over ten measurements. The FFT duration for the web algorithm [shown as N in (2)] is 3200 points and the sampling rate [$1/T_s$ in (2)] is 7.168 MHz. Traces (e)–(g) represent the errors in (a)–(c), respectively, with respect to (d) and are plotted on the right axis. The magnitude error is obtained in decibels as a ratio of the two magnitude measurements.

The error traces (f) and (g) for both magnitude and phase are comparable, i.e., when the signal-to-noise ratio is good, the errors can be attributed mostly to the channel mismatch in the vector spectrum analyzer (specified to be within ± 0.25 dB, $\pm 2^{\circ}$). The large errors shown in trace (e) are the result of poor signal-to-noise ratio above the 3-dB BW of the filter. As discussed earlier, this error can be reduced by increasing the duration of the matched filtering, or, equivalently, the frequency resolution of the FFT measurement.

V. Example 2

When the vector signal analyzer is used to generate arbitrary bandpass signals ($>$ 10 MHz) using the HP 89431A RF section, it is not possible to ensure synchronism between independent measurements. Thus, a Sony/Tektronix arbitrary waveform generator (AWG 520) was used as the exciting source. In this case, the digital marker output data of the AWG 520 was used to trigger the vector signal analyzer measurement (see Fig. 7). The lack of synchronization of sampling frequencies is overcome by using a Hanning window before performing the FFT. The AWG 520, the vector signal analyzer, and a PC are networked using the general-purpose interface bus (GPIB) and the measurements logged and processed by the PC. The source is compensated using the measurements on channel #1, as described in the previous example.

The filter measured in this case is a K & L bandpass filter at 100 MHz with a 10-dB BW of 6 MHz. Figs. 8 and 9 show the magnitude and phase measurements. Trace (a) is obtained using the web algorithm, while (b) was obtained using a network analyzer (HP4396B). Trace (c) represents the error in (a) with respect to (b). The network analyzer is configured to measure the response at 800 points and average the spectrum over 16 measurements (IF BW is 40 kHz), while the FFT duration for the web algorithm [shown as N in (2)] is 3200 points at a sampling rate [$1/T_s$ in (2)] of 15.36 MHz. The results are within the measurement error of the instruments used.

VI. Example 3

The Sony/Tektronix arbitrary waveform generator (AWG 520) operates at a sampling rate of 1 GS/s and, thus, the maximum frequency it can generate is 500 MHz. Hence, to measure filters above that frequency range, a frequency upconverter is used. In this example, a Mini Circuits quadrature modulator, i.e., ZAMIQ-895M, is used to upconvert the signal. The overall source is compensated using the measurement on channel #1 of the vector signal analyzer, as mentioned in Section IV.

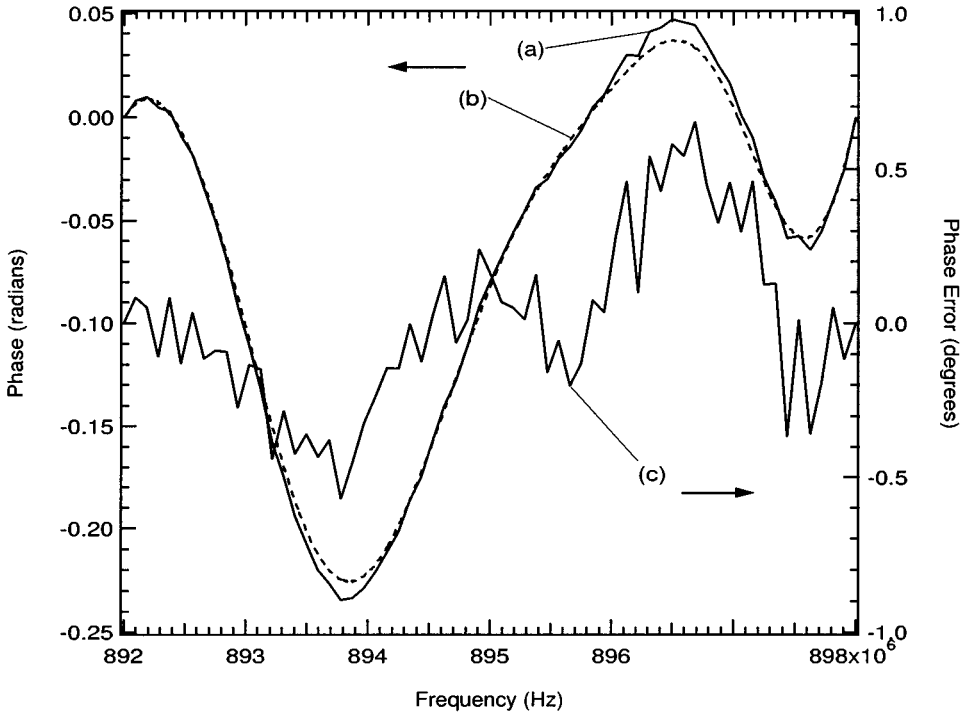

Fig. 11. Phase response of 895-MHz K & L bandpass filter. (a) Web algorithm (—). (b) Network analyzer HP8753E, (- - -). (c) Difference (a)–(b).

The vector signal analyzer restricted the measurable BW to 6 MHz. We used two tunable K & L bandpass filters with a nominal BW of 1% and slightly offset center frequencies around 895 MHz to create an interesting response for this measurement. The measured response is shown in Figs. 10 and 11. Trace (a) is obtained using the web algorithm and (b) is obtained using the network analyzer (HP8753E). Trace (c) represents the error in (a) with respect to (b). The network analyzer is configured to measure the response at 1600 points and average the spectrum over 16 measurements, while the web algorithm operates as described in Section V. The results are within the measurement error of the HP network analyzer.

VII. Conclusions

This paper has shown that it is possible to make both magnitude and phase measurements of a transmission path, with network analyzer accuracy, *in situ*, using a low-complexity compact measurement setup. Such *in situ* calibration can both improve system performance and relax temperature/time stability requirements of the components in the transmission path.

The basic ideas in this paper can also be extended in a straightforward way to make relative phase measurements between channels in a multichannel system by first summing the respective channels and then feeding them into the power detector. Thus, it is possible to generate any number of channels with precise amplitude and phase match. This multichannel technique can be applied with equal ease to baseband, RF, and optical systems.

References

[1] T. Lin and H. Samulei, "A 200-MHz CMOS $x/\sin(x)$ digital filter for compensating D/A converter frequency response distortion," *IEEE J. Solid-State Circuits*, vol. 26, pp. 1278–1285, Sept. 1991.

[2] B. G. Henriques and J. F. Franca, "High-speed D/A conversion with linear phase $\sin x/x$ compensation," in *Proc. IEEE Int. Circuits Syst. Symp.*, vol. 2, 1993, pp. 1204–1207.

[3] F. Harris, "Implementing waveform shaping filters to pre-equalize gain and phase distortion in the analog signal processing path in DSP based modems," in *Proc. IEEE MILCOM Conf.*, vol. 2, 1994, pp. 633–638.

[4] A. A. M. Saleh and J. Salz, "Adaptive linearization of power amplifiers in digital radio systems," *Bell Syst. Tech. J.*, vol. 62, no. 4, pp. 1019–1033, Apr. 1983.

[5] P. Kockaert, M. Peeters, S. Coen, P. Emplit, M. Haelterman, and O. Deparis, "Simple amplitude and phase measuring technique for ultra-high-repetition-rate lasers," *IEEE Photon. Technol. Lett.*, vol. 12, pp. 187–189, Feb. 2000.

[6] O. M. Collins and N. Vasudev, "The effect of redundancy on measurement," *IEEE Trans. Inform. Theory*, vol. 47, pp. 3090–3096, Nov. 2001.

N. Vasudev was born in Hyderabad, India. He received the B.E. degree (with honors) in instrumentation from the Birla Institute of Technology and Science, Pilani, India, in 1993, the M.S. degree in electrical engineering from the Indian Institute of Technology, Chennai, India, in 1997, and the Ph.D. degree in electrical engineering from the University of Notre Dame, Notre Dame, IN, in 2001.

He is currently a Design Engineer with Stryker Endoscopy, San Jose, CA. His research interests include communication systems and signal processing.

Oliver M. Collins (S'88–M'89–SM'99–F'02) was born in Washington, DC. He received the B.S. degree in engineering and applied science, and the M.S. and Ph.D. degrees in electrical engineering from the California Institute of Technology, Pasadena, in 1986, 1987, and 1989, respectively.

From 1989 to 1995, he was an Assistant Professor and then an Associate Professor in the Department of Electrical and Computer Engineering, Johns Hopkins University, Baltimore, MD. In September 1995, he became an Associate Professor in the Department of Electrical Engineering, University of Notre Dame, Notre Dame, IN. He became a Full Professor in 2001 and currently teaches courses in communications, information theory, coding, and complexity theory.

Dr. Collins was the recipient of the 1994 IEEE Thompson Prize Paper Award, the 1994 Marconi Young Scientist Award presented by the Marconi Foundation, and the 1998 IEEE Judith Resnik Award.